

Effects of particle sedimentation and rotation on axisymmetric gravity currents

Andrew J. Hogg^{a)}

Centre for Environmental and Geophysical Flows, School of Mathematics, University of Bristol, University Walk, Bristol BS8 1TW, United Kingdom

Marius Ungarish^{b)}

Department of Computer Science, Technion, Haifa 32000, Israel

Herbert E. Huppert^{c)}

Institute of Theoretical Geophysics, Department of Applied Mathematics and Theoretical Physics, University of Cambridge, Silver Street, Cambridge CB3 9EW, United Kingdom

(Received 22 February 2001; accepted 19 June 2001)

The axisymmetric propagation of a relatively dense gravity current of a given initial volume over a horizontal boundary is considered when the intruding fluid is a suspension of heavy particles and the ambient fluid is steadily rotating about a vertical axis. The investigation employs a shallow-water model of the motion. With the introduction of a strained temporal coordinate, it is possible to derive asymptotic expressions for the evolution of the radius and height of the current, the radial and temporal variation of the horizontal velocity, the volume fraction of particles, and the angular velocity. In this way it is possible to distinguish how the Coriolis force and the effects of particle sedimentation inhibit the radial spreading of the flow. The analytical relationships arise directly from the shallow-water equations and thus improve upon previous simple expressions which are based on an *a priori* prescription of the shape for the current. The analytical results compare favorably with both numerical integration of the full system of equations and experimental data. © 2001 American Institute of Physics. [DOI: 10.1063/1.1412244]

I. INTRODUCTION

When density-driven flows evolve in a rotating environment, the nature of their motion is very different from that which arises when the flow takes place in an otherwise quiescent environment. In the presence of rotation, Coriolis effects deflect the flow and the fluid is subject to centrifugal accelerations which inhibit radial spreading. For example, in a rotating system a lens of dense fluid becomes unstable to azimuthal motions which form discrete eddies on the length scale of the Rossby radius;¹ buoyant plumes also become unstable and break up into vortices;² and the rate of radial spreading of relatively dense fluid over a horizontal rigid boundary is progressively reduced.³

In this paper we study the axisymmetric propagation of a gravity current generated by the instantaneous release of relatively dense fluid. The motion is driven by the density difference between the intruding fluid and the surrounding ambient, an occurrence which is common in natural processes and industrial applications.⁴ The excess density of the intruding fluid may be due to compositional differences, such as a temperature or salinity, or may be due to the presence of relatively heavy particles in suspension, in which case the density difference is progressively reduced as the particles sediment to the underlying boundary. In a rotating environ-

ment Coriolis effects play a central role in the evolution of these gravity-driven flows. For example, large-scale turbidity currents which flow across the continental shelf, while driven by the presence of suspended particulate matter, are influenced by the effects of rotation. We note that the dynamics of axisymmetric releases of dense fluid differ from those that are laterally confined by a sidewall. For these latter flows, azimuthal motion is inhibited and the motion is predominantly parallel to the boundary.⁵

In this paper we develop a shallow-water model for the flow on the assumption that the depth of the current is much less than its length. We further assume that the current flows through deep ambient fluid so that the motion within the ambient can be neglected. By appropriate analysis of the physical processes governing the motion we identify a regime that is common in nature, in which the effects of particle sedimentation and ambient rotation are initially small. The initial motion is dominated by a dynamical balance between the buoyancy associated with the density difference and the inertia of the fluid. Within such a regime we find similarity solutions to the governing equations which model the initial motion.⁶ We then develop asymptotic series solutions which are appropriate to the regimes of slow particle sedimentation relative to the initial buoyancy-induced radial velocity and weak Coriolis effects relative to the initial hydrostatic, radial pressure gradients. These solutions demonstrate how each of the effects modifies the internal dynamics of the flow. Both physical processes lead to a reduction in flow speed relative to that in a compositionally driven cur-

^{a)}Electronic mail: a.j.hogg@bris.ac.uk

^{b)}Electronic mail: unga@csa.cs.technion.ac.il

^{c)}Electronic mail: hch1@esc.cam.ac.uk

rent propagating in the absence of rotation. However, the ways in which the flow adjusts to realize these reductions are quite different for each case. The theoretical developments show that particle sedimentation causes the tail of the current to thin as the particle-laden fluid accumulates close to the front. This effect was reported in the context of two-dimensional flows,⁷ where it was observed in experiments and numerical computations. The effects of Coriolis forces are compensated by a change in the profile of the current. It becomes “nose-down” to develop a streamwise pressure gradient. Such profiles are found in viscously dominated flows,⁸ in drag-affected inertial flows,⁹ and in flows within porous media.¹⁰

Our asymptotic expansions are based upon the new technique developed by Harris *et al.*¹¹ This technique has been shown to work well for flows which are two dimensional and nonrotating. In this study, we apply the technique to axisymmetric flows for which the details of the asymptotic expansion are quite different. The expansions indicate how the solutions gradually drift away from the similarity solution as the flow becomes no longer dominated by an inertial-buoyancy balance but instead is influenced by Coriolis effects and the progressive reduction of the buoyancy force through particle sedimentation. From the expansions we assess the relative magnitudes of these two effects by identifying appropriate dimensionless ratios. In previous studies of axisymmetric gravity currents,^{12,3,13} numerical integration of the governing equations has been required for each set of parameter values. This is avoided here because it is possible to derive closed form analytical expressions. A different approach, employed by Bonnacaze *et al.*¹² for particle-driven flows and by Ungarish and Huppert¹⁴ for rotating flows, is to formulate “box” models for the flow. These neglect the internal dynamics of the flow, but permit relatively simple analytical expressions for the radial speed to be derived. In this paper, since we develop solutions to more complete governing equations, we are able to assess the validity of these box models.

The paper is organized as follows. In Sec. II we formulate the problem and identify the dimensionless parameters that represent the relative magnitude of the Coriolis force to the inertia of the fluid and the magnitude of the settling velocity of the particles to the initial radial speed. We present the underlying similarity solution in Sec. III and then derive the asymptotic solutions in Sec. IV which are compared to results obtained from the numerical integration of the governing equations. Finally in Sec. V we discuss the results and compare them with the experimental work presented in Refs. 12 and 13. We also indicate how this analysis improves upon existing formulations and draw some conclusions about the internal dynamics of the flow.

II. FORMULATION

We consider the intrusion of a current of density ρ_c through an ambient fluid of a lower density ρ_a , which is rotating about a vertical axis at rate Ω (Fig. 1). The intruding current contains small, relatively heavy particles, all of the same size, which are suspended within a fluid of identical

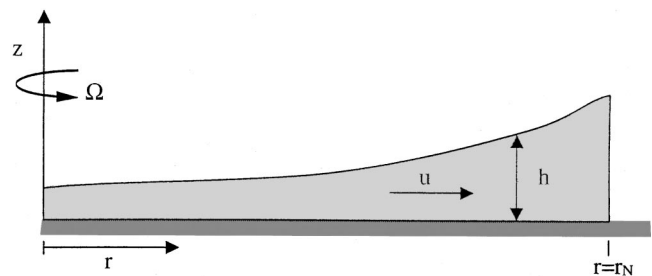


FIG. 1. Configuration of the flow.

density to the surrounding ambient. The density of the particles is ρ_p and they have volume fraction ϕ , which varies both spatially and temporally. The density of the current is given by

$$\rho_c = \rho_a + \phi(\rho_p - \rho_a). \quad (2.1)$$

The motion of the dense current is driven by the buoyancy force associated with the density difference between it and the ambient fluid. In this study we consider flows that possess an axisymmetric geometry and spread radially from a source. We assume that the horizontal length scale of the motion far exceeds that in the vertical and so there is negligible vertical acceleration. Thus we may employ a shallow-water model of the motion in which the pressure is a combination of hydrostatic and centrifugal terms. We adopt a cylindrical polar coordinate system in a frame which is fixed in the rotating frame of reference. We denote the vertical axes by z , the radial by r , and assume that there is no dependence upon the azimuthal coordinate (i.e., the flow is radially symmetric). Within the current, the pressure is given, up to an additive constant, by

$$p = \frac{1}{2}\rho_a\Omega^2r^2 + (\rho_p - \rho_a)g \int_z^h \phi dz - \rho_agz, \quad (2.2)$$

where h is the depth of the current. We formulate the shallow-water equations which describe the flow by considering the conservation of mass, momentum, and the transport of particles. We vertically average these equations on the assumption that the velocity of the current and the volume fraction of particles are vertically uniform through the depth of the current. This procedure is discussed thoroughly in the appendix to Harris *et al.*¹¹ and should be regarded as closure assumptions for the model. The assumption of the vertical distribution of the particulate phase implies that the intensity of the fluid turbulence must be sufficient to mix the particles vertically throughout the depth of the current but insufficient to re-entrain deposited particles from the underlying boundary. (An alternative, laminar model for the behavior of the particulate phase, in which the boundary of the current is defined by the uppermost sedimenting layer of particles, has been proposed by Ungarish and Huppert.³ In this view the volume fraction of particulate remains constant and equal to its initial value, but the fluid mass, moving with the current, is progressively reduced.) In our model, the vertically averaged expression of mass conservation, on the assumption that ambient fluid is not entrained into the current, is given by

$$\frac{\partial h}{\partial t} + \frac{1}{r} \frac{\partial}{\partial r} (ruh) = 0. \tag{2.3}$$

If viscous forces are negligible then the dynamics of the current are dominated by a balance between inertial, buoyancy and Coriolis forces. Utilizing the Boussinesq approximation that density variations are only important when multiplied by gravitational terms, we find that the radial momentum equation is given by

$$\frac{\partial}{\partial t} (uh) + \frac{1}{r} \frac{\partial}{\partial r} (ru^2h) + \frac{\partial}{\partial r} \left(\frac{1}{2} g' h^2 \right) = v h \left(2\Omega + \frac{v}{r} \right), \tag{2.4}$$

where u is the radial velocity, v is the azimuthal velocity, and $g' \equiv (\rho_c - \rho_a)g/\rho_a$ is the reduced gravity. The azimuthal momentum equation is given by

$$\frac{\partial}{\partial t} (vh) + \frac{1}{r} \frac{\partial}{\partial r} (ruvh) = -uh \left(2\Omega + \frac{v}{r} \right). \tag{2.5}$$

Finally the transport of particles may be expressed by^{12,3}

$$\frac{\partial}{\partial t} (h\phi) + \frac{1}{r} \frac{\partial}{\partial r} (ru\phi h) = -V_s \phi, \tag{2.6}$$

where V_s denotes the settling velocity of the particles.

The boundary conditions on this flow are that there is no radial flow and no radial gradient of angular velocity at the origin, which are expressed as

$$u(0,t) = 0, \quad \frac{\partial}{\partial r} \left(\frac{v}{r} \right) = 0 \quad \text{at } r=0. \tag{2.7}$$

At the front of the current there is a dynamic condition linking the frontal speed with the local velocity of long gravity waves. This condition, the Froude number condition, was established in the context of steady, two-dimensional flows by Benjamin;¹⁵ experimentally tested by Huppert and Simpson;¹⁶ and has been successfully utilized in a number of subsequent studies,^{12,3,17} to cite just a few. It has also been shown to be applicable to rotating systems.¹³ In the context of flows through relatively deep ambient fluid, the condition is given by

$$u = \text{Fr}(g'h)^{1/2} \quad \text{at } r=r_N(t), \tag{2.8}$$

where $r_N(t)$ denotes the radial front of the current and Fr is a constant, given by 1.19 when the depth of the ambient fluid is much greater than the depth of the current.¹⁶ In addition we express the global conservation of mass by

$$\int_0^{r_N} rh \, dr = \frac{1}{2} V, \tag{2.9}$$

where πV is the total volume of the dense fluid. To (2.7)–(2.9), we add initial conditions. In this study we employ the simple initial conditions appropriate to a “lock release.” This permits direct comparison with experiments.^{3,12,13} We thus write

$$u = v = 0, \quad h = h_0, \quad \phi = \phi_0 \quad \text{for } r < r_0 \quad \text{at } t = 0, \tag{2.10}$$

where $h_0 r_0^2 = V$.

Following Ungarish and Huppert,³ we note that the conservation of potential vorticity follows directly from (2.3), (2.5), and (2.10). We find that

$$\frac{D}{Dt} \left(\frac{\xi + 2\Omega}{h} \right) = 0, \tag{2.11}$$

where $D/Dt = \partial/\partial t + u\partial/\partial r$ and $\xi = (1/r)\partial(rv)/\partial r$ is the vertical component of the relative vorticity. Hence we deduce that potential vorticity is conserved on fluid particles. Thus, given the “lock-release” initial conditions, which imply that the potential vorticity is $2\Omega/h_0$ for all the fluid, and the boundary condition at the origin (2.7), we integrate (2.11) to find that

$$\omega \equiv \frac{v}{r} = -\Omega + \frac{2\Omega}{r^2 h_0} \int_0^r r' h(r', t) dr'. \tag{2.12}$$

Use of this identity leads to a reduction in the number of partial differential equations needed to model the flow and a considerable simplification of the analysis which follows.

Non-dimensionalization. The system of equations and initial conditions admits five external, dimensional parameters: Ω , V_s , h_0 , r_0 , and $g'_0 \equiv (\rho_p - \rho_a)\phi_0 g/\rho_a$, from which we can form three nondimensional measures to characterize the dynamical behavior. We choose the aspect ratio of the initial release, r_0/h_0 ; the Coriolis parameter (the inverse of the Rossby number),

$$C = \frac{\Omega r_0}{(g'_0 h_0)^{1/2}}, \tag{2.13}$$

which is the ratio of the strength of the azimuthal velocity Ωr_0 to the magnitude of the buoyancy-induced inertial velocity; and a dimensionless settling flux defined by

$$\beta = \frac{V_s r_0}{h_0 (g'_0 h_0)^{1/2}}, \tag{2.14}$$

which is the ratio of the initial vertical settling flux of particles to the initial radial volume flux of fluid. If all these parameters vanish then the system admits a similarity solution. If any of them is nonzero, however, then the similarity solution is no longer formally correct, but may nevertheless provide useful insight into the evolution of the flow. Hogg *et al.*¹⁸ investigate numerically the role of the initial aspect ratio on the propagation of two-dimensional gravity currents. They find that the numerically calculated solution to the shallow water equations rapidly adjusts to the similarity solution, a conclusion which is borne out by experimental measurements. In the analysis which follows we hence assume that the dynamics are essentially independent of the initial aspect ratio. Expressed another way, the theory is valid when $r_N \gg r_0$.

In the regime $C \ll 1$, the flow is initially dominated by a balance between inertial and buoyancy forces with rotation playing only a negligible role. However, as the dense fluid radially spreads and slow, the effects of rotation become no longer negligible and the dynamics undergo a transition. This is in contrast with the regime $C \gg 1$ for which Coriolis effects dominate the motion straightaway and there is little radial propagation of the front, relative to the initial radius of

the intrusion. Furthermore the radially symmetric motion becomes prone to azimuthal instabilities.¹ In the present study, motivated by observations of Gulf Stream rings and other geophysical phenomena, we focus on the regime $C \ll 1$.

We also study the regime $\beta \ll 1$, in which the initial settling flux of particles is much smaller than the initial radial flux of fluid. (Bonnecaze *et al.*¹² suggest a typical value of 0.005.) Settling of particles to the underlying boundary reduces the density difference between the current and the ambient and leads to a reduced buoyancy force. Thus the radial velocity is reduced. Note that the limit $\beta = 0$ corresponds to a current with a constant density, such as a saline fluid intruding through a fresh-water ambient.

We observe that there are two independent length scales in this problem, namely the initial height, h_0 , and the initial radius, r_0 , and that these combine to give the volume as $V = r_0^2 h_0$. At this stage of the analysis it is convenient to non-dimensionalize heights with respect to h_0 and radial distances with respect to r_0 . However, we show in the following that these factors only occur as the product $r_0^2 h_0$ and so the relevant length scale is $V^{1/3}$. This bears out the observation that the dynamics become independent of the initial aspect ratio of the release. (A similar result was obtained in the study of two-dimensional particle-driven gravity currents in which the important length scale is the square root of the volume per unit width.¹⁸)

We adopt the following scaling of the variables, where an asterisk denotes a dimensionless variable:

$$[h, u, v, \phi, r, t] = [h_0 h^*, (g_0' h_0)^{1/2} u^*, \Omega r_0 v^*, \phi_0 \phi^*, r_0 r^*, r_0 (g_0' h_0)^{-1/2} t^*]. \tag{2.15}$$

In what follows we omit the asterisk in the interests of clarity and assume that all variables are dimensionless. The equations governing the evolution of an inertial gravity current, driven by the presence of suspended particulate matter, undergoing rotation are given by

$$\frac{\partial h}{\partial t} + \frac{1}{r} \frac{\partial}{\partial r} (r u h) = 0, \tag{2.16}$$

$$\frac{\partial u}{\partial t} + u \frac{\partial u}{\partial r} + \phi \frac{\partial h}{\partial r} + \frac{h}{2} \frac{\partial \phi}{\partial r} = C^2 r \omega (\omega + 2), \tag{2.17}$$

$$\frac{\partial \phi}{\partial t} + u \frac{\partial \phi}{\partial r} = -\frac{\beta \phi}{h}, \tag{2.18}$$

$$\frac{\partial \omega}{\partial t} + u \frac{\partial \omega}{\partial r} = -2u(1 + \omega). \tag{2.19}$$

This system of equations is completed by the dimensionless boundary condition at the front of the current,

$$\frac{dr_N}{dt} = \text{Fr}(\phi h)^{1/2} \quad \text{at } r = r_N(t), \tag{2.20}$$

the conditions of symmetry at the origin

$$u = 0, \quad \frac{\partial \omega}{\partial r} = 0 \quad \text{at } r = 0, \tag{2.21}$$

and an expression for the conservation of fluid volume

$$\int_0^{r_N(t)} h r dr = \frac{1}{2}. \tag{2.22}$$

The conservation of potential vorticity leads to

$$\omega = -1 + \frac{2}{r^2} \int_0^r r' h(r', t) dr'. \tag{2.23}$$

III. SIMILARITY SOLUTION ($\beta = C = 0$)

In the limit $r_0/h_0 = C = \beta = 0$, the current maintains a constant density difference with the ambient ($\phi = 1$) and the azimuthal motion is decoupled from the radial motion. This solution is relevant to the propagation of an axisymmetric saline current through a nonrotating, fresh-water ambient. The similarity solution to these equations is given by

$$r_N = K t^{1/2}, \tag{3.1}$$

$$h = \frac{K^4}{8 r_N^2} (y^2 - 1 + 2/\text{Fr}^2), \tag{3.2}$$

$$u = \frac{dr_N}{dt} y, \tag{3.3}$$

where $y = r/r_N$ and $K = [16 \text{Fr}^2 / (4 - \text{Fr}^2)]^{1/4}$.^{6,12} When C and β are nonzero, but still much smaller than unity, this similarity solution describes the initial evolution of the current, before either rotation or particle sedimentation have had an effect on the motion. The effect of a nonzero, but finite aspect ratio is such that the flow is initially far from the similarity solution but rapidly converges to it over an initial ‘‘slumping phase’’ which is much shorter than the duration of the flows under consideration here.¹⁸ A similar phenomenon has recently been investigated in the context of draining flows within porous media.¹⁹

We assess the times at which rotation begins to influence the motion from (2.17) by balancing inertial and Coriolis terms using the similarity solution as estimates for the velocity and height fields. This requires that $C^2 r \omega h \sim u^2 h/r$. Estimating that $\omega \sim 1$ and $u \sim r/t$, we find that these are of equivalent magnitude when $C^2 t^2 = O(1)$. Similarly, we assess the times when particle sedimentation has begun to influence the motion from (2.18). Balancing sedimentation and particle advection gives $\beta \sim u h/r$. Hence particle sedimentation begins to play a significant role when $\beta t^2 = O(1)$. A straightforward, but limited expansion in powers of βt^2 was pursued by Hogg *et al.*¹⁸ in the context of axisymmetric, particle-driven currents. In Sec. IV we employ a different strategy which has the advantage over Hogg *et al.*¹⁸ that it yields convergent expansions which are valid even as the current approaches its maximum radial extent.

IV. POWER-SERIES EXPANSIONS

The system of equations is currently presented with r and t as the independent variables. We change variables to a nonlinear function of time, s , and a scaled spatial coordinate, η , such that the current occupies $0 \leq \eta \leq 1$. Thus, we substitute

$$\eta = r/r_N(t), \tag{4.1}$$

and, following the technique of Harris *et al.*,¹¹ we introduce a nonlinear function of time, s , which is related to the radius of the current, $r_N(t)$, at time t by

$$s = [r_N(t)/a]^m, \quad \frac{ds}{dt} = s^n F(s). \tag{4.2}$$

Here a , m , and n are constants, to be determined in the following, and $F(s)$ is a regular function of s such that $F(0) = 1$. This technique is similar to the method of strained coordinates.²⁰ We choose the constants a , m , and n such that together with the leading-order term of the straining function, $F(0) = 1$, we recover the similarity solution for the rate of propagation and the height and horizontal velocity fields within the current (see Sec. III). Thereafter the effects of particle sedimentation and the Coriolis force alter the dynamics of the flow and lead to the current diverging from its similarity form. It is convenient to write the dependent variables in terms of (η, s) in the forms

$$h(r, t) = a^m H(s, \eta)/r_N(t)^2, \quad u(r, t) = \frac{dr_N}{dt} U(s, \eta). \tag{4.3}$$

In what follows we will develop asymptotic power series for the dependent variables which are essentially valid for $C^2 s \ll 1$ and $\beta s \ll 1$, on the assumption that the leading terms in the expansions are the similarity solutions of Sec. III. We deduce the value of a by requiring that $F(0) = 1$ and the values of m and n by balancing the terms within the governing equations and boundary conditions. From the dynamic boundary condition (2.20), we find that $m(1 - n) = 2$; while from (2.18), we find that $mn = 2$. Hence we deduce that $m = 4$ and $n = 1/2$. [Note that the perturbation driven by the Coriolis term in (2.17) implies that $2n = 1$, which is consistent with the values deduced from balancing the terms in the particle-transport equation.]

We are now in a position to derive the equations of motion in terms of the new dependent variables η and s . After considerable algebra, we find that

$$4s \frac{\partial H}{\partial s} - \left(2H + \eta \frac{\partial H}{\partial \eta} - \frac{1}{\eta} \frac{\partial}{\partial \eta} (\eta U H) \right) = 0, \tag{4.4}$$

$$\begin{aligned} \frac{sF^2}{4} \frac{\partial U}{\partial s} + \left(-\frac{F}{16} + \frac{s}{4} \frac{dF}{ds} \right) FU + \frac{F^2}{16} \left((U - \eta) \frac{\partial U}{\partial \eta} \right) \\ + \phi \frac{\partial H}{\partial \eta} + \frac{H}{2} \frac{\partial \phi}{\partial \eta} = C^2 s \eta \omega (2 + \omega), \end{aligned} \tag{4.5}$$

$$sF \frac{\partial \phi}{\partial s} + \frac{F}{4} (U - \eta) \frac{\partial \phi}{\partial \eta} = -\frac{\beta \phi s}{a^2 H}. \tag{4.6}$$

Conservation of potential vorticity, following (2.23), may be expressed as

$$\omega = -1 + \frac{2a^2}{s^{1/2} \eta^2} \int_0^\eta H(s, \eta') \eta' d\eta'. \tag{4.7}$$

Also conservation of fluid volume is given by

$$a^4 \int_0^1 H(s, \eta) \eta d\eta = \frac{1}{2}. \tag{4.8}$$

The boundary conditions are now more simply expressed as

$$U(s, 0) = 0, \quad U(s, 1) = 1. \tag{4.9}$$

These represent zero flow at the origin and a kinematic condition at the front of the flow, respectively. The other boundary condition is now given by

$$F(s) = 4 \text{Fr}[H(s, 1) \phi(s, 1)]^{1/2}. \tag{4.10}$$

We pose series solutions in ascending powers of s for each of the functions in the revised governing equations. We demonstrate in the following that the leading order in the expansion corresponds to the similarity solution of Sec. III. The effects of particle sedimentation and rotation are then treated as perturbations to this similarity solution. At leading-order their effects are independent and may be combined linearly. We thus find terms of order $C^2 s$ and βs in the power series expansion. (At higher orders their effects are no longer independent.) It is convenient to define $\bar{\beta} = \beta/a^2$ and pose power series of the form

$$\begin{aligned} H(s, \eta) = H_0(\eta) + \bar{\beta} s H_{P1}(\eta) + C^2 s H_{R1}(\eta) \\ + O(C^4 s^2, \bar{\beta} C^2 s^2, \bar{\beta}^2 s^2), \end{aligned} \tag{4.11}$$

$$\begin{aligned} U(s, \eta) = U_0(\eta) + \bar{\beta} s U_{P1}(\eta) + C^2 s U_{R1}(\eta) \\ + O(C^4 s^2, \bar{\beta} C^2 s^2, \bar{\beta}^2 s^2), \end{aligned} \tag{4.12}$$

$$\begin{aligned} \phi(s, \eta) = 1 + \bar{\beta} s \phi_{P1}(\eta) + C^2 s \phi_{R1}(\eta) \\ + O(C^4 s^2, \bar{\beta} C^2 s^2, \bar{\beta}^2 s^2), \end{aligned} \tag{4.13}$$

$$F(s) = 1 + \bar{\beta} s F_{P1} + s C^2 F_{R1} + O(C^4 s^2, \bar{\beta} C^2 s^2, \bar{\beta}^2 s^2), \tag{4.14}$$

where the subscripts P and R denote functions and values associated with the effects of particulate matter and rotation, respectively. We note that the relative importance of the Coriolis force to the change in buoyancy due to particle sedimentation is measured by the magnitude of $C^2/\bar{\beta}$ as identified by Ungarish and Huppert¹⁴ from other considerations. In terms of dimensional parameters

$$\frac{C^2}{\bar{\beta}} = a^2 \left(\frac{\Omega^4 V}{V_s^2 g'_0} \right)^{1/2}. \tag{4.15}$$

Hence the relative magnitude of the effects of the Coriolis force and particle sedimentation are independent of the initial aspect ratio, but depend on the volume of fluid released. We also note that there can be no $O(C^2)$ term in the volume fraction expansion since there is no particle settling at this order and so $\phi_{R1} = 0$. Therefore an $O(C^4 s^2)$ correction also vanishes from this expansion. We substitute these power series into the governing equations and equate terms in equal powers of s .

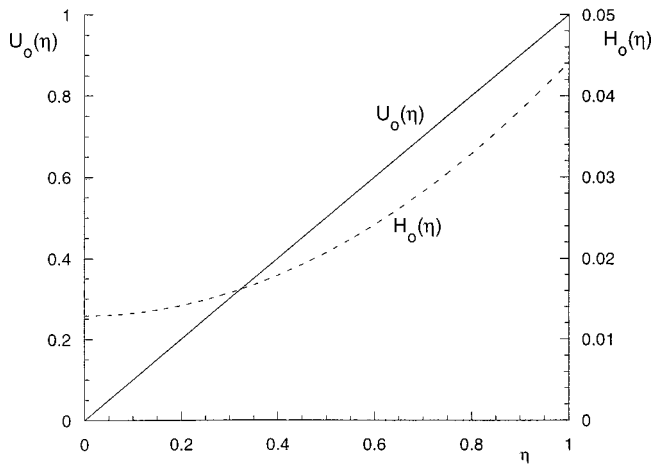


FIG. 2. Similarity solution for an axisymmetric gravity current of constant density in a nonrotating environment. The velocity field, $U_0(\eta)$ (—) and the height field, $H_0(\eta)$ (---).

A. Similarity solution: $O(1)$ terms

The solution at $O(1)$ is given by

$$H_0(\eta) = \frac{1}{32} \left(\eta^2 + \frac{2}{Fr^2} - 1 \right), \tag{4.16}$$

$$U_0(\eta) = \eta, \tag{4.17}$$

and a is determined from the conservation of fluid volume and is given by

$$a = \left(\frac{64 Fr^2}{4 - Fr^2} \right)^{1/4}. \tag{4.18}$$

Hence $a = 2.43$ for $Fr = 1.19$. These functions are identical to the similarity solution presented in Sec. III (Fig. 2). For the rotating current we derive from (4.7)

$$\omega = -1 + \frac{a^2}{32s^{1/2}} \left(\frac{\eta^2}{2} + \frac{2}{Fr^2} - 1 \right). \tag{4.19}$$

B. Particle-driven currents: $O(\bar{\beta}s)$ terms

On substitution of the power series (4.11)–(4.14) into the governing equations and equating terms of $O(\bar{\beta}s)$, we find that

$$4H_{P1}\eta + (\eta U_{P1}H_0)' = 0, \tag{4.20}$$

$$\frac{1}{4}U_{P1} + H'_{P1} + \frac{1}{2}H_0\phi'_{P1} + \phi_{P1}H'_0 = -\frac{1}{8}F_{P1}\eta, \tag{4.21}$$

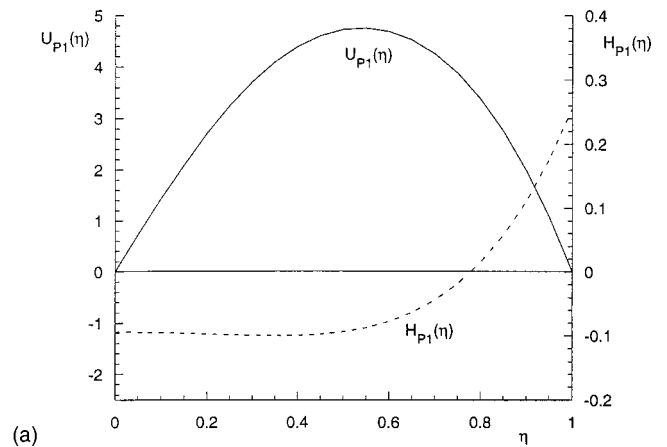
$$\phi_{P1} = -\frac{1}{H_0}, \tag{4.22}$$

where a prime denotes differentiation with respect to η . The boundary conditions are

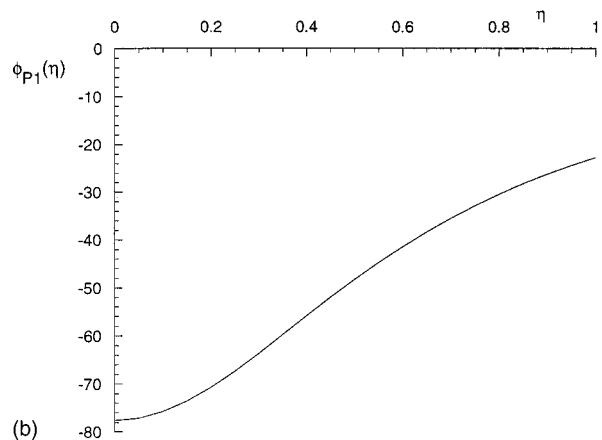
$$U_{P1}(0) = 0, \quad U_{P1}(1) = 0. \tag{4.23}$$

Furthermore from the Froude number condition (4.10), we deduce that

$$\frac{H_{P1}(1)}{H_0(1)} = 2F_{P1} - \phi_{P1}(1). \tag{4.24}$$



(a)



(b)

FIG. 3. (a), (b) First-order perturbation functions for the velocity (—), height (---), and volume fraction (—) as a function of the similarity variable η . These functions represent the correction to the similarity solution due to particle sedimentation.

We combine Eqs. (4.20)–(4.22) into a single equation for $H_{P1}(\eta)$, which admits the analytical solution

$$H_{P1}(\eta) = -\frac{1}{16} + \frac{F_{P1}}{6\eta} (\eta^2 H_0)' + \alpha {}_2F_1[(1 - \sqrt{33})/2, (1 + \sqrt{33})/2; 1; -\eta^2/(-1 + 2/Fr^2)], \tag{4.25}$$

where ${}_2F_1$ denotes a hypergeometric function²¹ and α is a constant which has yet to be determined. On application of the boundary conditions (4.23) and (4.24), we find that

$$\alpha = 4.52 \times 10^{-3}, \quad F_{P1} = -8.42 \quad \text{for } Fr = 11.9. \tag{4.26}$$

Subsequent terms in this expansion may be determined by substituting into the governing equations and equating appropriate powers of $\bar{\beta}s$. However, the complexity of the algebra prevents the identification of an analytical solution, although we note that the second-order perturbation to the volume fraction, $\bar{\beta}^2 s^2 \phi_{P2}(\eta)$, is given by

$$\phi_{P2} = \frac{1}{2H_0} \left(-F_{P1} - \frac{U_{P1}H'_0}{4H_0} + \frac{1}{H_0} + \frac{H_{P1}}{H_0} \right). \tag{4.27}$$

We plot the functions $H_{P1}(\eta)$, $U_{P1}(\eta)$, and $\phi_{P1}(\eta)$ in Fig. 3. Particle sedimentation means that the radial speed of the current is reduced ($F_{P1} < 0$) as the density difference

between the current and the ambient is progressively reduced. However the sedimentation is not uniform throughout the flow. Instead a greater proportion of the particles settle in the region of the origin, where the current is thinner. In its initial similarity state, the radial gradient of the hydrostatic pressure increases linearly so that fluid is decelerated as it approaches the front. The dominant effect of sedimentation in the tail of the current is that this adverse pressure gradient is reduced. Therefore the fluid accelerates toward the front and the current thickens. We note that similar interpretation of the dynamics of the flow is noted by Bonnecaze *et al.*⁷ and emerges from the expansions employed by Hogg *et al.*¹⁸

C. Rotating currents: $O(C^2s)$ terms

We derive the perturbation solutions due to the effects of rotation in an analogous manner to Sec. IV B, although in this case the azimuthal velocity drives the correction to the momentum equation (2.17) and the volume fraction of particles remains constant. From (4.19) we determine that

$$\omega = -1 + O(s^{-1/2}) \tag{4.28}$$

and hence on substitution of the power series into the governing equations and equating terms of $O(C^2s)$ we find that

$$4H_{R1}\eta + (\eta U_{R1}H_0)' = 0, \tag{4.29}$$

$$\frac{1}{4}U_{R1} + H'_{R1} = -\frac{1}{8}F_{R1}\eta - \eta, \tag{4.30}$$

$$\phi_{R1} = 0. \tag{4.31}$$

Equation (4.31) expresses the conservation of the volume fraction of particles. The boundary conditions are given by

$$U_{R1}(0) = 0, \quad U_{R1}(1) = 0. \tag{4.32}$$

Furthermore, from the Froude number condition (4.10), we deduce that

$$\frac{H_{R1}(1)}{H_0(1)} = 2F_{R1}. \tag{4.33}$$

As before, we combine (4.29)–(4.31) into a single equation for $H_{R1}(\eta)$, which admits the analytical solution

$$H_{R1}(\eta) = \left(1 + \frac{F_{R1}}{8} \right) \frac{3}{2\eta} (\eta^2 H_0)' + \gamma_2 \mathcal{F}_1 \left[(1 - \sqrt{33})/2, \right. \\ \left. \times (1 + \sqrt{33})/2; 1; -\eta^2 / (-1 + 2/Fr^2) \right], \tag{4.34}$$

where γ is an undetermined constant. On application of the boundary conditions we find that

$$\gamma = -2.40 \times 10^{-3}, \quad F_{R1} = -1.28 \quad \text{for} \quad Fr = 1.19. \tag{4.35}$$

As before, we generate subsequent terms in this expansion by substitution into the governing equations and balancing terms of the same order. We note that if the volume fraction is expressed by $\phi = 1 + \bar{\beta}\phi_{P1} + \bar{\beta}^2\phi_{P2} + \bar{\beta}C^2\phi_{R2} + \dots$, then

$$\phi_{R2} = \frac{1}{2H_0} \left(\frac{H_{R1}}{H_0} - \frac{U_{R1}H_0'}{4H_0} + F_{R1} \right). \tag{4.36}$$

We plot the functions $H_{R1}(\eta)$ and $U_{R1}(\eta)$ in Fig. 4. The main effect of rotation is to slow the current relative to its speed of radial spreading in the absence of rotation (F_{R1}

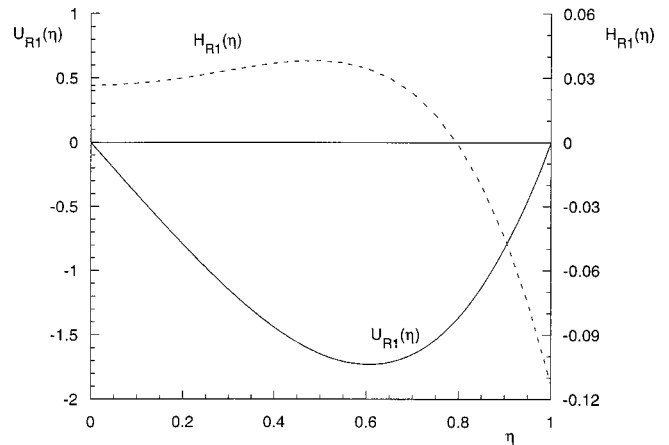


FIG. 4. First-order perturbation functions for the velocity (—) and height (---) as a function of the similarity variable η . These functions represent the correction to the similarity solution due to rotation.

<0). The magnitude of this inhibiting force, though, increases with distance from the origin. In order that the current may continue to propagate, it develops a radial pressure gradient to counteract the Coriolis force. Its profile therefore becomes “nose-down,” as observed by Ref. 13 and as predicted from the shape of $H_{R1}(\eta)$. This means that at a finite time the front of the current will touch the underlying boundary [$h(r_N, t) = 0$]. Thereafter the model presented here will no longer be valid. The dynamic boundary condition at the front of the current is then inappropriate and the flow may start to radially contract.¹³ In assessing the accuracy of the asymptotic expansion, it is only relevant to consider times up to when the nose first touches the boundary.

In terms of the power series developed here, truncated at $O(s)$, the angular velocity is given by

$$\omega = -1 + \frac{2a^2}{\eta s^{1/2}} \left(\frac{1}{32} \left(\frac{1}{4} \eta^3 + \frac{1}{2} \eta (-1 + 2/Fr^2) \right) \right. \\ \left. - \frac{1}{4} \bar{\beta} s U_{P1}(\eta) H_0(\eta) - \frac{1}{4} C^2 s U_{R1}(\eta) H_0(\eta) + \dots \right). \tag{4.37}$$

D. Comparison with numerical results

To validate the series expansion solutions, we compare the asymptotic results with those calculated from the numerical integration of the governing equations (2.3)–(2.6). A full description of the numerical method employed is given in Ungarish and Huppert.³ Essentially the partial differential equations were integrated using a two-step Lax–Wendroff scheme to which a small amount of artificial viscosity was added to the momentum equation to ensure numerical stability. The method is explicit and so a small time step is required, but even then the run times are only of the order of a few seconds on a Silicon Graphics Octane workstation. Since the objective of these numerical runs is to verify the asymptotic expansion, the initial conditions employed were the similarity solution at $t = 2$.

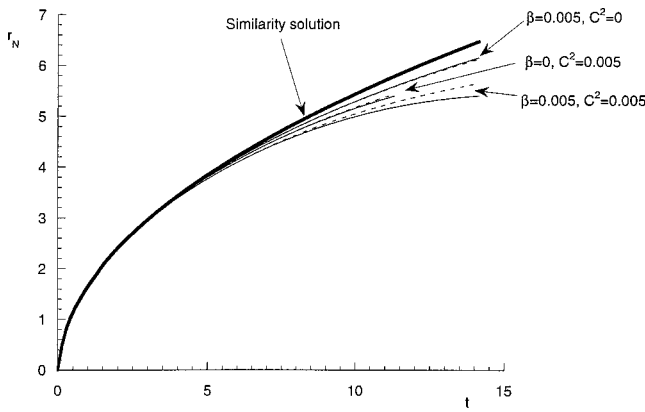


FIG. 5. The radial extent of the gravity current as a function of time. Shown are: the similarity solution ($\beta=0, C^2=0$); and solutions for $\beta=0.005, C^2=0$; $\beta=0, C^2=0.005$; and $\beta=0.005, C^2=0.005$. The numerically calculated results (—); the asymptotic results (---).

In order to compare the asymptotic and numerical solutions of the shallow water equations, we must invert the relationship between the strained coordinate, $s(t)$, and time. Recall that we have found that

$$\frac{ds}{dt} = s^{1/2}(1 + \bar{\beta}sF_{P1} + C^2sF_{R1} + \dots). \quad (4.38)$$

We truncate the series expansion for $F(s)$ at $O(s)$ and integrate (4.38) subject to the boundary condition $s(0)=0$. This yields

$$r_N(t) \equiv as^{1/4} = a \left[(-\bar{\beta}F_{P1} - C^2F_{R1})^{-1/2} \times \tanh \left(t \frac{(-\bar{\beta}F_{P1} - C^2F_{R1})^{1/2}}{2} \right) \right]^{1/2}. \quad (4.39)$$

We plot $r_N(t)$ as a function of t for various values of β and C^2 in Fig. 5 and compare the asymptotic results with those from the numerical integration of the equations of motion. First note the progressive divergence of the solutions from the similarity solution ($\beta=0, C^2=0$). The effects of rotation and particle sedimentation are to slow the radial spreading of the current. The asymptotic expression captures the numerically determined behavior to a high degree of accuracy. The two are indistinguishable for currents in the absence of rotation ($C^2=0$). When some rotation of the ambient is included ($C^2>0$) there is a small discrepancy between the asymptotic and numerical results which increases with time. At late times, however, the nose of the gravity current has touched the boundary $h(r_N, t)=0$ and so the model presented here becomes invalid.

In terms of dimensional variables, (4.39) is given by

$$r_N = a \left(-\frac{F_{P1}V_s}{a^2V^{3/2}g_0'^{1/2}} - \frac{F_{R1}\Omega^2}{g_0'V} \right)^{-1/4} \times \tanh^{1/2} \left[\frac{t}{2} \left(\frac{-F_{P1}V_s g_0'^{1/2}}{a^2V^{1/2}} - F_{R1}\Omega^2 \right)^{1/2} \right]. \quad (4.40)$$

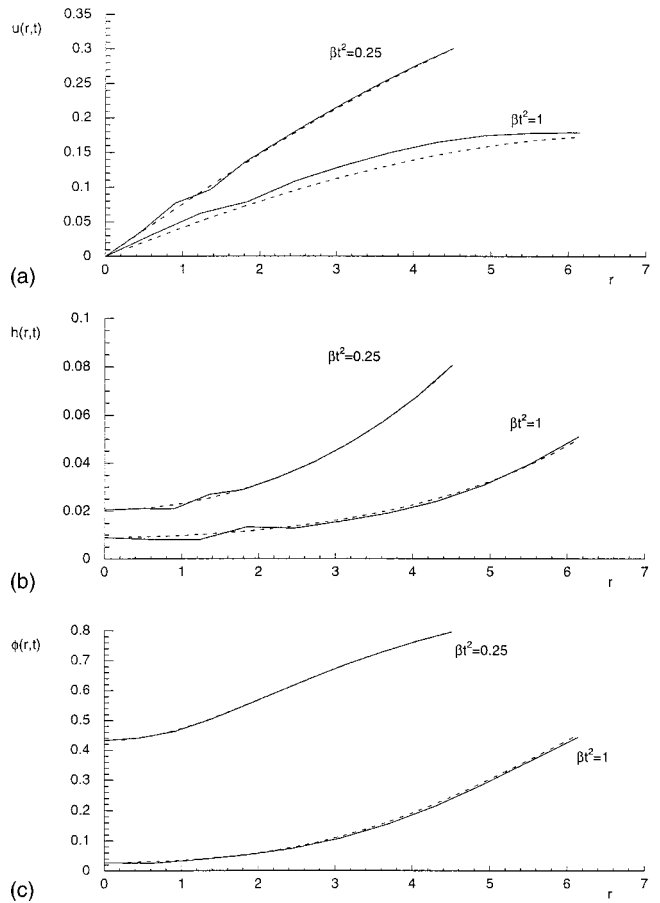


FIG. 6. (a)–(c) Comparison between the numerical results and the asymptotic theory at $\beta t^2=0.25$ and $\beta t^2=1$ for a particle-driven axisymmetric gravity current ($\beta=0.005$) in the absence of rotation ($C=0$). The numerical results (—); the asymptotic results (---).

Note that as indicated in Sec. II, this expression depends upon the length scales r_0 and h_0 through the product $V = r_0^2 h_0$.

We now compare the asymptotic expressions and the numerical-evaluated profiles for the velocity, height, particle volume fraction, and azimuthal angular velocity at two times and for three pairs of values of β and C^2 (Figs. 6–8). For the rotating flows, the later time shown in Figs. 7 and 8 is $Ct = 0.8$, which corresponds to approximately one-fifth of a revolution of the system. By this stage we anticipate that rotational effects will have strongly influenced the dynamics of the flow. Hence we expect significant departure from the nonrotating similarity solution. In Figs. 6–8 we have not plotted the straightforward series expansion for the volume fraction $(1 + \bar{\beta}s\phi_{P1} + \bar{\beta}^2\phi_{P2} + \bar{\beta}C^2\phi_{R2})$. Instead, following Ref. 11, we have derived an improved expression for the volume fraction of particles. Rather than treating ϕ as a power series in s and using Padé approximants to improve convergence, we seek an expression for ϕ of the form

$$\bar{\phi} = (1 + \bar{\beta}sF_{P1} + \bar{\beta}^2s^2b(\eta))^{-1/H_0(\eta)F_{P1}}, \quad (4.41)$$

where $b(\eta)$ is yet to be determined. This expression arises from balancing the unsteady term, $sF(s)\partial\phi/\partial s$, with the sedimentation term $-\bar{\beta}s\phi/H_0(\eta)$. By writing $F(s)=1$

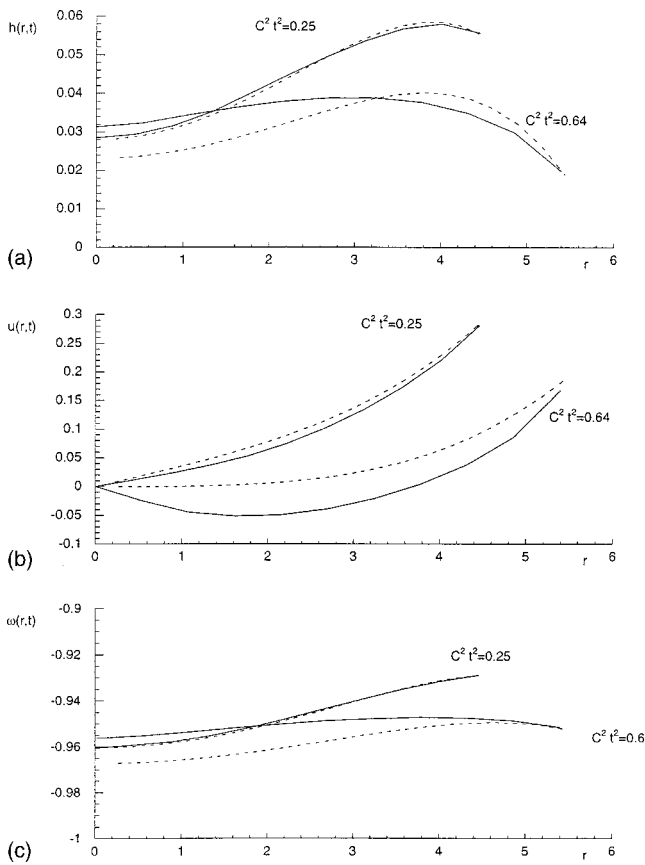


FIG. 7. (a)–(c) Comparison between the numerical results and the asymptotic theory at $C^2 t^2 = 0.25$ and $C^2 t^2 = 0.64$ for a constant density axisymmetric gravity current ($\beta = 0$) in a rotating environment ($C^2 = 0.005$). The numerical results (—); the asymptotic results (---).

+ sF_{P1} and integrating, we anticipate a function of the form (4.41). The function, $b(\eta)$, is found by projecting the Taylor expansion of (4.41) onto the power series expansion for ϕ up to and including the terms of $O(s^2)$. In this way we find that

$$b(\eta) = \frac{F_{P1}}{8H_0} (U_{P1}H'_0 - 4H_{P1}) + \frac{C^2 F_{P1}}{8\bar{\beta}H_0} (U_{P1}H'_0 - 4H_{R1} - 4F_{R1}H_0). \quad (4.42)$$

We observe that the theory developed here provides a very accurate representation of the numerical results for particle-driven currents in the absence of rotation (Fig. 6). At the later time ($\beta t^2 = 1$), approximately 95% of the particles have sedimented out of the flow and yet the asymptotic expressions provide an excellent representation of the flow structure. This agreement is a considerable improvement upon the expansions employed by Ref. 18. For the gravity currents with rotation (Figs. 7 and 8), the agreement between the numerical and series solutions is good, although there are significant differences with the internal structure of the velocity field at the later time ($Ct = 0.8$). The numerical calculations find an extensive region of reverse radial flow ($u < 0$), which is not found by the series solution. The other characteristics of height, volume fraction of particles, and

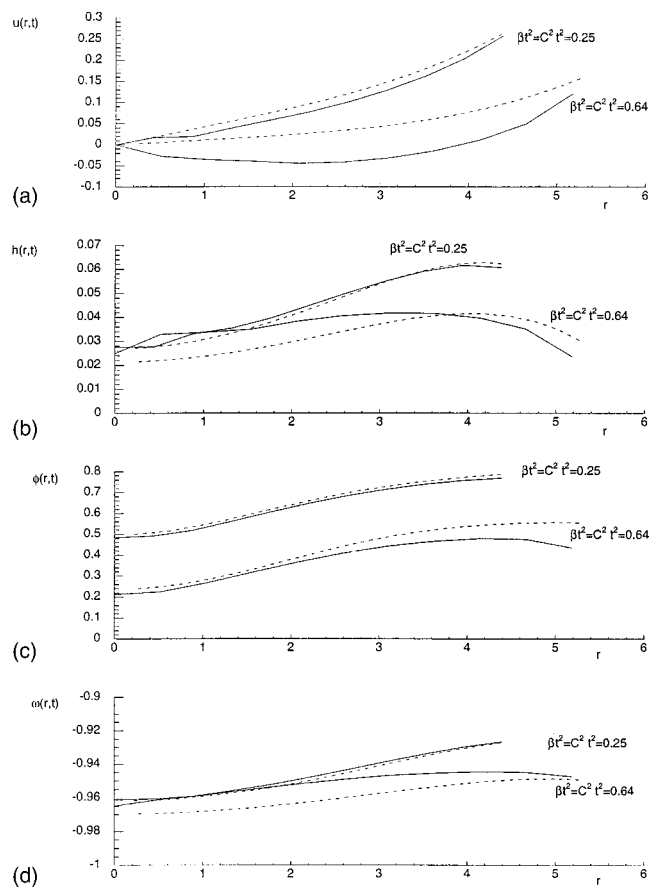


FIG. 8. (a)–(d) Comparison between the numerical results and the asymptotic theory at $\beta t^2 = C^2 t^2 = 0.25$ and $\beta t^2 = C^2 t^2 = 0.64$ for a particle-driven axisymmetric gravity current ($\beta = 0.005$) in a rotating environment ($C^2 = 0.005$). The numerical results (—), the asymptotic results (---).

angular velocity, however, do exhibit good agreement between the numerical and asymptotic results. We note that at times just in excess of those shown in Figs. 7 and 8 ($Ct \approx 0.92$), the nose of the current touches the boundary and so it is no longer possible to use the model presented here for this flow. Instead a new frontal boundary condition is required, as suggested by Ungarish and Huppert.³

The model proposed for the nonrotating, particle-driven currents is valid until either the particles have all settled out of suspension or until viscous forces have become non-negligible. The radial velocity is always positive and the flow attains a maximum extent. Thus the introduction of the strained temporal coordinate is a suitable choice of independent variable. For the rotating current, however, the nose of the current touches the boundary at a finite time and thereafter the imposed boundary condition at the front becomes invalid. At this time we expect that the leading order term in the height field, H_0 , is of comparable magnitude with the perturbation due to rotation, $C^2 s H_{1R}$. Thus the expansion is no longer asymptotic. This is borne out by the comparison between asymptotic theory and numerical calculation described previously. However, we find by trial and error that a good way to improve the expansions is to expand in terms of $C^2 t^2$ and $\bar{\beta}s$, rather than $C^2 s$ and $\bar{\beta}s$. We convert the ex-

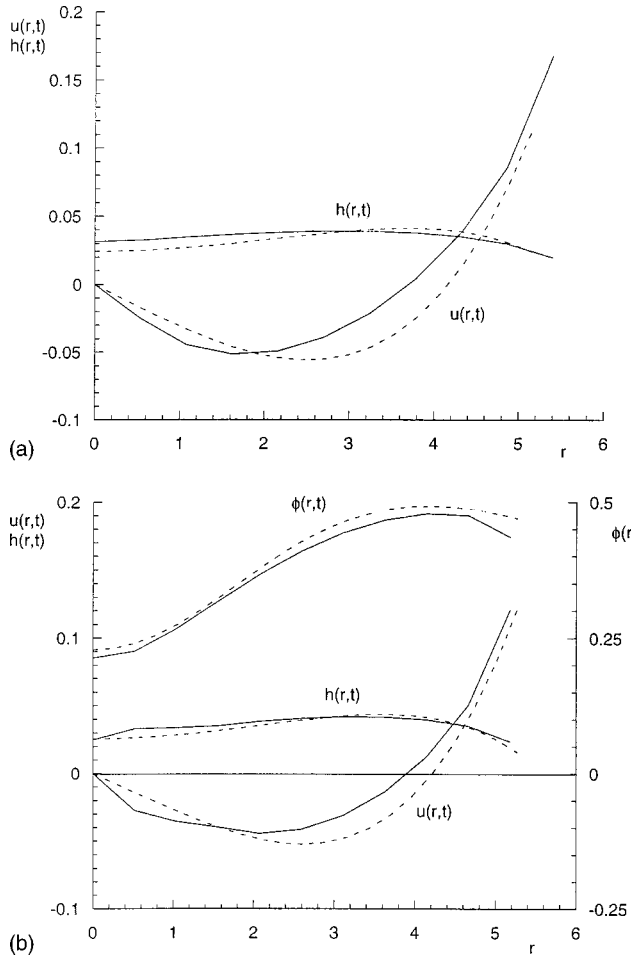


FIG. 9. Comparison between the numerical results and the improved asymptotic theory at $t=11.3$ for (a) constant density axisymmetric gravity current ($\beta=0$) in a rotating environment ($C^2=0.005$); and (b) particle-driven axisymmetric gravity current ($\beta=0.005$) in a rotating environment ($C^2=0.005$). The numerical results (—); the asymptotic results (---).

pansions developed here into this form by writing $s = C^2 t^2/4 + \dots$ and hence we find that

$$H(s, \eta) = H_0(\eta) + \bar{\beta} s H_{P1}(\eta) + C^2 (t/2)^2 H_{R1}(\eta) + \dots, \quad (4.43)$$

$$U(s, \eta) = U_0(\eta) + \bar{\beta} s U_{P1}(\eta) + C^2 (t/2)^2 U_{R1}(\eta) + \dots, \quad (4.44)$$

$$\frac{dr_N}{dt} = \frac{1}{4s^{1/2}} (1 + \bar{\beta} s F_{P1} + C^2 (t/2)^2 F_{R1}), \quad (4.45)$$

$$b(\eta) = \frac{F_{P1}}{8H_0} (U_{P1} H_0' - 4H_{P1}) + \frac{C^2 t^2 F_{P1}}{32\bar{\beta} H_0} (U_{R1} H_0' - 4H_{R1} - 4F_{R1} H_0). \quad (4.46)$$

We plot in Fig. 9 the asymptotic and numerical results at $t=11.3$ using these alternative expressions and note that the agreement between them is improved.

TABLE I. The initial conditions of the axisymmetric lock-release gravity currents in a rotating environment (after Ref. 13). The depth of the ambient fluid is denoted by H .

Experiment	r_0 (cm)	h_0 (cm)	H (cm)	g' (cm s^{-2})	Ω (s^{-1})	C
R4	100	46.4	80.3	19.24	0.050	0.17
R5	100	46.6	80.1	19.04	0.100	0.34
R9	100	46.2	79.5	42.36	0.150	0.34
R10	100	46.3	80.0	9.80	0.050	0.23
R12	100	47.0	82.9	9.41	0.050	0.24
R15	100	46.7	81.7	24.14	0.078	0.23
R16	100	16.7	82.1	23.94	0.078	0.39
R17	100	48.0	83.2	23.94	0.078	0.23

V. DISCUSSION

Both the effects of particle sedimentation and rotation result in a reduction in the speed of radial spreading of the gravity current. However, the detailed ways in which the internal dynamics adjust to achieve this is different in each case. In the former case, particle sedimentation leads to an overall reduction of buoyancy and so the radial speed is reduced. However, sedimentation is greatest close to the origin where the depth of the flow is least. The current was initially in a similarity state in which the pressure gradient balances the inertia of the flow and increases linearly with distance from the source. Thus sedimentation reduces the density difference between the current and the ambient and so leads to a weakening of this pressure gradient close to the source. Hence the adverse, radial pressure gradient is reduced and the fluid accelerates toward the front of the current where it accumulates [Fig. 3(a)]. The first-order perturbation height, H_{P1} , is thus negative close to the origin and positive close to the front; the current propagates “nose” up. Conversely, the effects of rotation lead to a reduction in radial velocity throughout the current and a depletion of fluid at the front as the current develops a radial pressure gradient to balance the Coriolis force. The fluid is therefore decelerated and the first-order height, H_{R1} , is positive close to the origin and negative close to the front; the current propagates “nose” down.

We now compare the results from our asymptotic model with experimental data of intrusions of saline solution into a rotating, fresh-water ambient¹³ and of intrusions of relatively dense, particle-laden fluid through a quiescent ambient.¹²

Ungarish *et al.*¹³ conducted experiments within a 13.0-m-diam, 1.2-m-deep cylindrical tank, mounted on a platform which rotated about a vertical axis at a rate in the range $0.05\text{--}0.15\text{ s}^{-1}$. They released saline solutions into the main body of fluid, from within a centrally located inner cylinder of radius 1 m. The intruding solution had initial values of the reduced gravity in the range $9.4\text{--}42.4\text{ cm s}^{-2}$. The radial extent of the saline solution was measured as a function of time for a range of different initial conditions (see Table I). In the absence of particles ($\bar{\beta}=0$) and in terms of dimensional variables, (4.39) is given by

$$r_N(t) = a \left(\frac{g_0' V}{-F_{R1} \Omega^2} \right)^{1/4} \tanh^{1/2} \left(\frac{(-F_{R1})^{1/2} \Omega t}{2} \right). \quad (5.1)$$

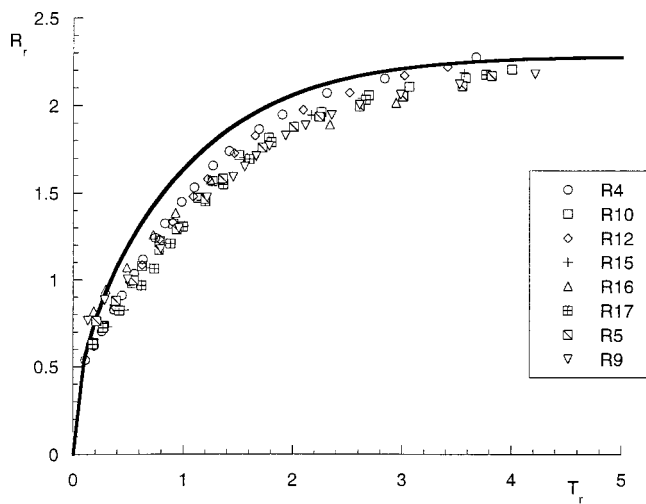


FIG. 10. Experimental results of Ungarish *et al.* (Ref. 13) for the radius of a saline intrusion within a rotating environment as a function of time. Here the radius and time are rendered dimensionless with respect to $(g'_0 V / \Omega^2)^{1/4}$ and Ω^{-1} , respectively. The theoretical prediction (—).

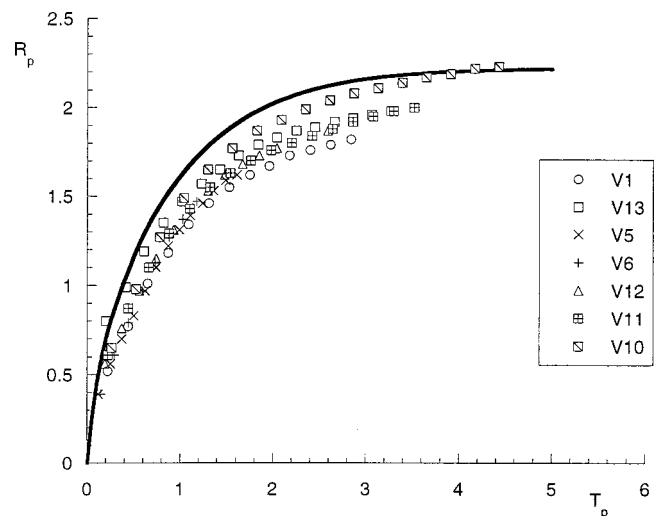


FIG. 11. Experimental results of Bonneau *et al.* (Ref. 12) for the radius of an intrusion of suspended particles within a nonrotating environment as a function of time. Here the radius and time are rendered dimensionless with respect to $(g'_0 V^3 / V_s^2)^{1/8}$ and $(g'_0 V^2 / V_s)^{-1/4}$, respectively. The theoretical prediction (—).

Hence we plot the experimental data in terms of the new dimensionless variables,

$$R_r = r_N \left(\frac{g'_0 V}{\Omega^2} \right)^{-1/4}, \quad T_r = \Omega t. \quad (5.2)$$

We note that $R_r = r_N C^{1/2} / r_0$ and observe from Fig. 10 that this scaling has collapsed the experimental data. Furthermore the theoretical predictions using the values $a = 2.43$ and $F_{R1} = -1.28$ agree favorably with the experimental measurements.

Bonneau *et al.*¹² performed experiments on the axisymmetric propagation of particle-laden fluid through a nonrotating, fresh water ambient. Their experiments were conducted in radial sector tanks. Measured quantities of silicon carbide particles were suspended in water and released from behind a lock gate at the apex of the sector tank. The particles have a density of 3.2 g cm^{-3} and those with an average diameter of either 23 or $37 \text{ }\mu\text{m}$ were employed in their study. Two radial sector tanks were employed with half-angles of 4° and 5° . The radial extent of the intruding suspension as a function of time was measured for a range of initial concentration of suspended particles and initial volumes (see Table II). On the assumption that the radial boundaries of the sector

tanks do not strongly influence the dynamics of the flow, these currents should evolve in an analogous way to those which originate from a truly axisymmetric source. In the absence of rotation ($C^2 = 0$) and in terms of dimensional variables, (4.39) is given by

$$r_N(t) = a \left(\frac{a^2 g'_0{}^{1/2} V^{3/2}}{-F_{P1} V_s} \right)^{1/4} \tanh^{1/2} \left[\frac{t}{2} \left(\frac{-F_{P1} V_s g'_0{}^{1/2}}{a^2 V^{1/2}} \right)^{1/2} \right]. \quad (5.3)$$

Hence we plot the experimental data in terms of the following new dimensionless variables:

$$R_p = r_N \left(\frac{g'_0{}^{1/2} V^{3/2}}{-F_{P1} V_s} \right)^{-1/4}, \quad T_p = t \left(\frac{V_s g'_0{}^{1/2}}{V^{1/2}} \right)^{1/2}. \quad (5.4)$$

We observe from Fig. 11 that this scaling has collapsed the experimental data. Furthermore the theoretical predictions using the values $a = 2.43$ and $F_{P1} = -8.42$ agree favorably with the experimental measurements.

We emphasize that there are no free parameters in this model other than the Froude number at the front, which has been empirically determined by experiments within a nonrotating channel.¹⁶ There are a number of ways in which the

TABLE II. The initial conditions of the axisymmetric lock-release gravity currents, driven by a suspension of particles in a nonrotating environment (after Ref. 12). The depth of the ambient fluid is equal to the initial depth of the lock (h_0). These experiments were performed in a sector tank of angle θ .

Experiment	θ ($^\circ$)	V (cm^3)	h_0 (cm)	ϕ_0 ($\times 10^{-2}$)	g'_0 (cm s^{-2})	V_s (cm s^{-1})	β ($\times 10^{-3}$)
V1	8	1585	14	1.92	41.8	0.123	3.9
V5	8	1585	14	0.97	21.1	0.056	2.5
V6	8	1585	14	1.92	41.8	0.056	1.8
V10	8	777	14	1.92	41.8	0.123	2.7
V11	8	777	14	0.97	21.1	0.123	3.8
V12	8	777	14	0.49	10.6	0.123	5.4
V13	10	1167	15	0.87	18.9	0.123	4.3

experimental conditions differ from the assumptions underlying the model developed here. First, the depth of the ambient does not greatly exceed the depth of the current, especially so at the early stages of the evolution of the current and so the Froude number should be weakly dependent upon the relative depths. Furthermore, the currents start from a lock of relatively large aspect ratio and so there will be a time of adjustment while the flow is influenced by its initial conditions. Also it was not possible to remove the lock gate instantaneously and its removal may have some influence on the initial propagation of the current. Finally, the theory neglects the effects of viscosity on the flow, whereas these laboratory experiments will eventually become affected by viscous forces. Nevertheless, given these differences between the assumptions underlying the theory and the experimental conditions, the comparison between the two is very encouraging.

It is interesting to compare this analysis with some reduced models of axisymmetric gravity currents. Bonneau *et al.*¹² propose a “box” (integral) model for particle-driven flows. This model entails the horizontal averaging of the internal properties of the current and thus treating the current as uniform within a cylindrical shape which evolves in time. Although rather different in its theoretical basis, the relationship they derived for r_N as a function of time is identical to (4.39) with $C^2=0$ up to some multiplicative constants. Ungarish and Huppert¹⁴ develop reduced models for the effects of rotation on particle-driven flows. They also adopt an integral model but assume that the current is a conical shape so that the effects of the Coriolis force may be balanced by a radial hydrostatic pressure gradient. This permits the identification of the ratio C^2/β in determining whether the flow is more strongly influenced by the effects of sedimentation or rotation. What we have demonstrated in this study is that it is possible to derive approximate models of the flow directly from the shallow water equations by systematic expansions. These emerge as asymptotic solutions of the full system of shallow-water equations and in addition to providing an equation for the rate of radial growth of the dense fluid, it is also possible to calculate how the radial velocity, volume fraction of particles, angular velocity, and height of the intruding dense fluid vary with radial distance and how they evolve temporally. The considerable advantage that this model offers is that it is no longer necessary to assume the current adopts a specific shape. Instead the shape is explicitly calculated.

ACKNOWLEDGMENTS

The authors gratefully acknowledge the able assistance of Mark Hallworth in the analysis of the experimental data.

A.J.H. acknowledges the financial support of the Nuffield Foundation (NUF-NAL) and the EPSRC. M.U. acknowledges the support of the EPSRC and the Fund for the Promotion of Research at the Technion.

- ¹R. W. Griffiths and P. F. Linden, “The stability of vortices in rotating, stratified fluid,” *J. Fluid Mech.* **105**, 283 (1981).
- ²J. M. W. Bush and A. W. Woods, “Vortex generation by line plumes in a rotating stratified fluid,” *J. Fluid Mech.* **388**, 289 (1999).
- ³M. Ungarish and H. E. Huppert, “The effects of rotation on axisymmetric gravity,” *J. Fluid Mech.* **362**, 17 (1998).
- ⁴J. E. Simpson, *Gravity Currents in the Environment and the Laboratory* (Cambridge University Press, Cambridge, 1997), 244 pp.
- ⁵R. W. Griffiths, “Gravity currents on rotating systems,” *Annu. Rev. Fluid Mech.* **18**, 59 (1986).
- ⁶D. P. Hault, “Oil spreading on the sea,” *Annu. Rev. Fluid Mech.* **2**, 341 (1972).
- ⁷R. T. Bonneau, H. E. Huppert, and J. R. Lister, “Particle-driven gravity currents,” *J. Fluid Mech.* **250**, 339 (1993).
- ⁸H. E. Huppert, “The propagation of two-dimensional and axisymmetric viscous gravity currents over a rigid horizontal surface,” *J. Fluid Mech.* **121**, 43 (1982).
- ⁹L. Hatcher, A. J. Hogg, and A. W. Woods, “The effects of drag on turbulent gravity currents,” *J. Fluid Mech.* **416**, 297 (2000).
- ¹⁰H. E. Huppert and A. W. Woods, “Gravity-driven flows in porous layers,” *J. Fluid Mech.* **292**, 53 (1995).
- ¹¹T. C. Harris, A. J. Hogg, and H. E. Huppert, “A mathematical framework for the analysis of particle-driven gravity currents,” *Proc. R. Soc. London, Ser. A* (to be published).
- ¹²R. T. Bonneau, H. E. Huppert, and J. R. Lister, “Axisymmetric particle-driven gravity currents,” *J. Fluid Mech.* **294**, 93 (1995).
- ¹³M. Ungarish, M. A. Hallworth, and H. E. Huppert, “Axisymmetric gravity currents in a rotating system: Experimental and numerical investigations,” *J. Fluid Mech.* (submitted).
- ¹⁴M. Ungarish and H. E. Huppert, “Simple models of coriolis-influenced axisymmetric particle-driven gravity currents,” *Int. J. Multiphase Flow* **25**, 715 (1999).
- ¹⁵T. B. Benjamin, “Gravity currents and related phenomena,” *J. Fluid Mech.* **31**, 209 (1968).
- ¹⁶H. E. Huppert and J. E. Simpson, “The slumping of gravity currents,” *J. Fluid Mech.* **99**, 785 (1980).
- ¹⁷M. A. Hallworth, A. J. Hogg, and H. E. Huppert, “Effects of external flow on compositional and particle gravity currents,” *J. Fluid Mech.* **359**, 109 (1998).
- ¹⁸A. J. Hogg, M. Ungarish, and H. E. Huppert, “Particle-driven gravity currents: Asymptotic and box-model solutions,” *Eur. J. Mech. B/Fluids* **19**, 139 (2000).
- ¹⁹D. Pritchard, A. W. Woods, and A. J. Hogg, “On the slow draining of a gravity current moving through a layered porous medium,” *J. Fluid Mech.* **444**, 297 (2001).
- ²⁰M. J. Lighthill, “A technique for rendering approximate solutions to physical problems uniformly valid,” *Philos. Mag.* **40**, 1179 (1949).
- ²¹G. B. Arfken and H. J. Weber, *Mathematical Methods for Physicists*, 4th ed. (Academic, New York, 1995), 1029 pp.